Adapting Optimal Velocity Tracking Control To Account for WEC Constraints and Power-Take-Off Efficiencies [*]

Adam Stock [*] Nathan Tom [**] Carlos Gonzalez [***]

[*] *Wind Energy and Control Centre, University of Strathclyde, Glasgow, Scotland, G1 2TB, UK (e-mail: adam.stock@strath.ac.uk).*
[**] *National Renewable Energy Laboratory, Golden, CO 80401 USA (e-mail: nathan.tom@nrel.gov)*
[***] *Renewable Dynamics, 50 Richmond Street, Glasgow, G1 1XP, UK, (e-mail: carlos.gonzalez@renewable-dynamics.com)*

Abstract: Wave energy converters (WECs) come in many different forms, from point absorbers and oscillating water columns to bulge wave devices. This paper focuses on the control of point absorber WECs, which typically have a narrow-banded frequency response and, therefore, control is well placed to improve the energy capture of such WECs. The acausal nature of the control problem means that, theoretically optimal control is almost impossible to achieve in practice; however, optimal velocity tracking (OVT) offers a simple and robust approximation to optimal control that can achieve better power capture than passive linear damping methods, albeit with necessarily higher force demands. OVT is a form of impedance matching and the magnitude of the power-take-off (PTO) force demand is often not linearly proportional to the WEC velocity, which can lead to PTO force and speed combinations far from the optimal PTO efficiency. The highly nonlinear PTO force and speed to efficiency mapping can, without remedial measures, severely diminish the effectiveness of OVT techniques. In this paper, improvements to OVT are made, particularly regarding the limits on motion. In particular, a limit on acceleration is added and drift of the position when the acceleration and/or velocity are limited is prevented through the addition of a new integral term. An anti-wind up methodology to prevent controller integral wind up is also included. These additions allow OVT to be more easily applied in practice. The effect of PTO efficiency is explored, and a novel potential solution to the problem of adapting control to account for efficiency is presented. Both aspects of the work presented highlight the requirement for co-design of the WEC, PTO, and controller.

Keywords: Wave energy, optimal control, system constraints, conversion efficiency, sensitivity.

1. INTRODUCTION

One of the most common and well-studied WEC designs is the point absorber, which typically has a narrow-banded response, and so control is well placed to improve the energy capture (Ringwoord et al. (2014); Hals et al. (2011)). WEC optimal control theory is clearly the target for a control system; however, in practice optimal control is nearly impossible to achieve as it requires perfect knowledge of the future wave elevation because of the acausal nature of wave energy converter dynamics (Coe et al. (2017)). One methodology for approximate optimal control is optimal velocity tracking (OVT) (Fusco and Ringwood (2013)). As part of the Wave Energy Scotland Control Systems Call, the Integrated Marine Point Absorber Control Tool (IMPACT) was developed, which simplifies implementation of an OVT controller for WECs (Stock et al. (2018)). As part of IMPACT, four WECs were developed, which are dynamically similar to commercial point absorbers. The work in this paper uses the "WEC 2" model, a large, single-body, subsurface heaving point absorber WEC with a rated power of 3 MW. The power take-off (PTO) was

modelled based on the Trident Power-pod that was originally designed for use with linear damping (resistive) control methodologies. In order to provide the required power rating, 18 sets of 6 LGF30 PTOs were used, allowing for a peak force of 3.24 MN (Trident Energy (2014)). It should be noted that the PTO is well designed for linear damping methods but has not been adapted for OVT.

The control problem then becomes that of generating an accurate reference velocity signal and designing a controller that will minimise the error in velocity through actuation of the PTO force. A simple but effective methodology of achieving this goal was developed in Fusco and Ringwood (2013) as shown in Fig. 1. Whilst previous work in the field has made great advances in developing controller implementations that allow approximate optimal controllers to be designed and tested, the WECs in which these control methodologies are tested tend to be simple, and real-world complications, such as constraints on the position, velocity, acceleration, and force, are not considered. Often, efficiency is also neglected or is assumed to have a constant value across all operational conditions (Falcao and Henriques (2015)). In this paper, the OVT methodology of Fusco and Ringwood (2013) is further developed for a WEC with more complex hydrodynamics and with a PTO with defined efficiency curves and defined constraints on position, velocity, acceleration, and force. The methods for adapting the controller for constraints are presented in Section 3 and possible methods for adapting the controller to account for efficiency are presented in Section 4. A discussion of the implications for the design of WECs, PTOs, and future controllers is presented in section 5.

2. MATHEMATICAL MODELLING

For a heaving wave energy converter, with other modes of motion constrained, the linear hydrodynamic heave equation of motion can be modelled in the frequency domain by the follow expression (Falnes (2002)):

$$Z_3(\omega)\dot{\zeta}_3(\omega) = F_{ex}(\omega) + F_u(\omega) \qquad (1)$$

$$Z_3(\omega) = \lambda_{33}(\omega) + j\omega\left[M + \mu_{33}(\omega) - K_{33}/\omega^2\right] \qquad (2)$$

where $Z_3(\omega)$ is the WEC heave intrinsic impedance, ω is the wave angular frequency, $\dot{\zeta}_3(\omega)$ is the WEC heaving velocity, $F_{ex}(\omega)$ is the heave incident wave force, $F_u(\omega)$ is the control force acting on the WEC by the PTO system, λ_{33} is the hydrodynamic heave radiation wave damping, M is the WEC mass, μ_{33} is the hydrodynamic heave radiation added mass, and K_{33} is the linearized heave hydrostatic restoring coefficient.

Optimal WEC control can be achieved when the commanded PTO force is equal to the negative complex conjugate of the WEC intrinsic impedance multiplied by the WEC velocity (Falnes (2002)):

$$F_u(\omega) = -Z_3(\omega)^*\dot{\zeta}_3(\omega) \qquad (3)$$

An equivalent formulation for optimal WEC control is that the velocity of the WEC should follow the reference velocity given by:

$$v_{ref}(\omega) = \frac{F_{ex}(\omega)}{2\lambda_{33}(\omega)} = \frac{F_{ex}(\omega)}{H(\omega)} \qquad (4)$$
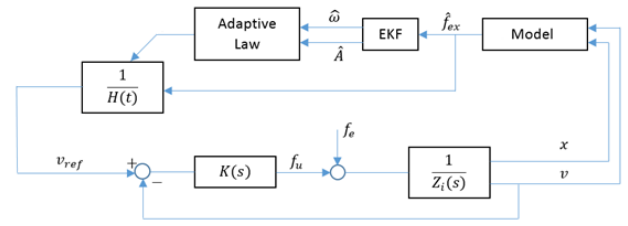

Fig. 1. Schematic of optimal velocity tracking control based on the Fusco and Ringwood methodology

Since the hydrodynamic heave radiation wave damping is a nonzero real valued number, then Eqn. 4 shows that the optimum WEC velocity will be in phase with the incident wave force and the oscillation amplitude will vary with wave frequency. To implement this optimal control strategy, an extended Kalman Filter is used to estimate the dominant frequency and amplitude of the heave wave-excitation force, which are then used as inputs to an adaptive law that sets the value of the gain, $1/H(\omega)$. The gain represents an estimate of $1/2\lambda_{33}(\omega)$ and multiplying the excitation force estimate by the gain produces a reference velocity for the controller to track. A controller is then designed to minimise the error between the measured velocity and reference velocity. In Fusco and Ringwood (2013), the WEC is modeled as a second-order system and the controller can be defined using the impedance of the WEC to calculate an appropriate controller transfer function. As part of the aforementioned IMPACT project, a controller design tool was developed that allows the the design of controllers for systems with more complex dynamics - this method was used in the work presented here (Stock et al. (2018)).

3. CONSTRAINING POSITION, VELOCITY, ACCELERATION, AND FORCE

The PTO force required to match the reference velocity, described by Eqn. (3) and Eqn. (4) respectively, assumes no system constraints; however, physical constraints, such as stroke length, limit the oscillation amplitudes required for maximum power capture, which can be a problem at longer wave lengths (Evans (1976)). The OVT methodology must be adapted to observe system constraints that will impact the maximum power capture, as discussed in Evans (1981).

3.1 Movement constraints

Constraint of the PTO position and velocity was presented in Fusco and Ringwood (2013) and the methodology is used here and extended to include acceleration limits, collectively referred to as movement constraints. The WEC reference velocity is given by:

$$v_{ref}(\omega) = \frac{F_{ex}(\omega)}{H(\omega)} \qquad (5)$$

and assuming that the excitation force is a narrow-band harmonic process with amplitude A, the complex magnitude of the velocity, $\hat{V}$, and position, $\hat{X}$, can be expressed as:

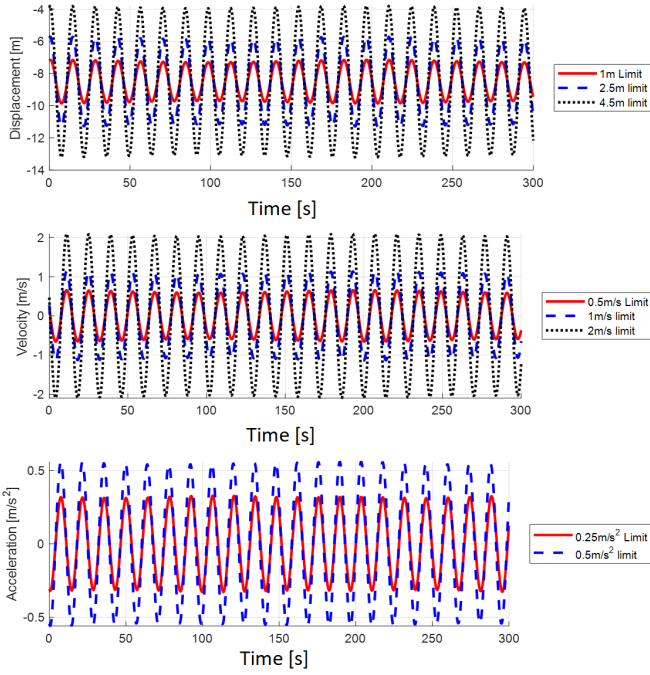$$\hat{V} = \frac{A}{H}e^{j\phi} \qquad (6)$$

Fig. 2. Application of various position, velocity, and acceleration limits for the IMPACT Exemplar WEC 2 under regular wave excitation with a 4.5-m wave height and 14-s period

$$\hat{X} = \frac{\hat{V}}{j\omega} = \frac{Ae^{j\phi}}{j\omega H} \quad (7)$$

When $\hat{X}$ is constrained:

$$\hat{X} = \frac{\hat{V}}{j\omega} < X_{lim} \rightarrow |\hat{V}| < X_{lim}\omega$$

$$\rightarrow \frac{A}{H} < X_{lim}\omega \rightarrow \frac{1}{H} < \frac{X_{lim}\omega}{A} \quad (8)$$

which gives an upper limit of the function $1/H$. Limits on the velocity and the acceleration can be applied using the same reasoning, with each giving an upper limit of $1/H$. Considering velocity:

$$|\hat{V}| = \frac{A}{H} < V_{lim} \rightarrow \frac{1}{H} < \frac{V_{lim}}{A} \quad (9)$$

Considering acceleration:

$$\hat{A}_{cc} = \hat{V}_{lim}j\omega \quad (10)$$

$$|\hat{V}|\omega = \frac{A}{H} < A_{cclim} \rightarrow \frac{1}{H} < \frac{A_{cclim}}{A\omega} \quad (11)$$

As more than one limit may be effective at any one time, the minimum value of $\frac{X_{lim}\omega}{A}$, $\frac{V_{lim}}{A}$, and $A_{cclim}A\omega$ is multiplied by the excitation force to produce the reference velocity that complies with the constraints. It should be noted that the formulation of the constraints given here assumes that the wave frequency and amplitude are known and correct but are normally estimated. As such, the constraints should not be used as hard constraints and an error margin must be considered. Fig. 2 shows examples of limiting the position, speed and acceleration of the WEC under regular wave excitation.

3.2 Force constraints

In addition to the limits on position, velocity, and acceleration, the command force must also be limited as PTOs have maximum and minimum forces that they can safely deliver. Whilst a simple saturation could be applied to the output from the controller, such a limit may lead to integral wind up if there is integration in the controller. To avoid integral wind up, a discrete form of anti-wind up is used. First, the transfer functions in the controller are defined in discrete form, such that:

$$F_s(s) \rightarrow F_z(z) = \frac{n(z)}{d(z)}$$

$$= \frac{a_{nz}^{-n} + a_{n-1}z^{n-1} + \ldots + a_1 z^{-1} + a_0}{b_{mz}^{-m} + b_{m-1}z^{-(m-1)} + \ldots + b_0 z^{-1} + 1} \quad (12)$$

$$F_z(z) - a_0 = z^{-1}\frac{m(z)}{d(z)} = z^{-1}G_z(z) \quad (13)$$

so,

$$f_k = g_{k-1} + a_0 u_k \quad (14)$$

In this way, the output of the function F at time step k is equal to the output of function G at the time step $k-1$ plus a constant times the input at time step k. Anti-wind up is usually applied using a feedback loop, wherein the feedback is proportional to the error between the variable to be limited and its maximum value. However, using the discrete method described here, instead of a large gain in a feedback loop, the equivalent of an infinite gain is implemented and so, in the case of the force demand exceeding the maximum value, the input to the controller is modified such that the force is exactly its maximum value. In Fig. 3, an example of the force limit is shown. Note that the force is successfully limited to the maximum value. A simulation with a pure saturation limit (no anti-wind up) is also shown for comparison of the effects of the anti-wind-up loop. It should be noted that, whilst not demonstrated here, the same methodology could be used to limit the rate of change of force if it was of concern. It is found that when the force limit is applied, the mean displacement of the device can drift substantially from the desired level during irregular wave simulations. In order to prevent this slow movement away from the desired depth, an addition is made to the controller that acts on the integral of the measured speed such that the error $\epsilon = v_{ref} - v$, is replaced by:

$$\epsilon = v_{ref} - v - \frac{kv}{s} \quad (15)$$

where k is a small number of the order of 0.05. The addition of the $\frac{kv}{s}$ term with a small K can be viewed as adding a very slow control action acting on mean displacement. Keeping the gain low prevents the addition from interfering with the controller action as the displacement component only acts at very low frequencies. The drift and the correction for it is also shown in Fig. 3. Note that the anti-wind up and drift correction improve the power capture, though the effect is small at around 1%.
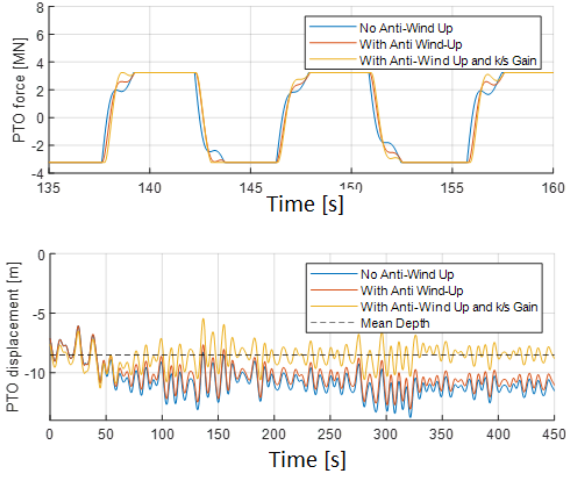
Fig. 3. Force and displacement with differing force limit methods with a 5-m wave height and 13-s period

4. ADAPTATIONS TO ACCOUNT FOR EFFICIENCY

Controllers for industrially developed point absorber WECs have, in the past, tended to be linear damping controllers. As such, many PTOs have been well designed to meet the demands of a passive linear damping (PLD) control methodology, with a constant (and high) efficiency along a linear mapping between velocity and force. The gradient of the linear relationship is often chosen to match the relationship between velocity and force from the optimum response of the WEC at its resonant frequency. However, for OVT methodologies, such a design may be far from optimal, as the desired phase response changes with wave frequency. An example of WEC-Sim outputs for the exemplar WEC 2 with the Trident power pod shown in Fig. 4 clearly highlights how the efficiency of a PTO designed for PLD has the effect that, although mechanical energy capture is higher with OVT, the electrical power output is lower, and, in some conditions, negative (i.e., power is consumed rather than generated). The magnitude and phase relationship of the PTO force-to-velocity transfer function for OVT can be expressed by the following:

$$F_V\left(\omega\right) = \frac{F_u\left(\omega\right)}{\dot{\zeta}_3\left(\omega\right)} = -Z_3^* \tag{16}$$

$$= -\lambda_{33}\left(\omega\right) + j\omega\left[\left(M_{33} + \mu_{33}\left(\omega\right)\right) - K_{33}/\omega^2\right]$$

$$|F_V\left(\omega\right)| = \sqrt{\Re\left\{-Z_3^*\left(\omega\right)\right\}^2 + \Im\left\{-Z_3^*\left(\omega\right)\right\}^2} \tag{17}$$

$$\angle F_V\left(\omega\right) = \arctan\left(\frac{\Im\left\{-Z_3^*\left(\omega\right)\right\}}{\Re\left\{-Z_3^*\left(\omega\right)\right\}}\right) \tag{18}$$

$$= \arctan\left(-\frac{\omega\left[M_{33} + \mu_{33}\left(\omega\right)\right] - K_{33}/\omega}{\lambda_{33}\left(\omega\right)}\right)$$

The phase angle between the PTO force and WEC velocity is bounded between $\pi/2$ and $3\pi/2$ and crosses π at the resonance frequency of the WEC. As shown in Fig. 5, calculated for WEC 2, the phase angle of the optimal PTO force-to-velocity transfer function deviates from π, which corresponds to PLD. The linear trace between the WEC velocity to PTO force for PLD is no longer optimum and becomes more oblong as the ratio of the imaginary-to-real
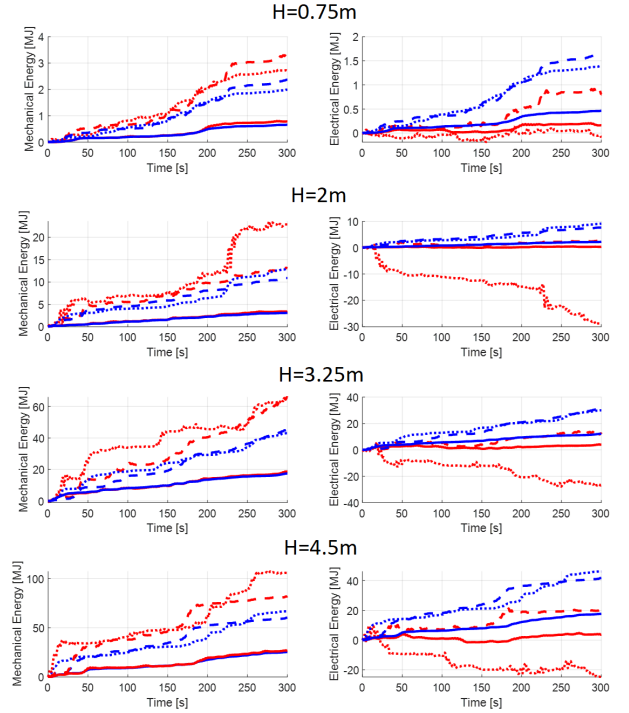

Fig. 4. Energy capture at various wave heights, H, for OVT (red) and PLD (blue) at periods of 5 s (solid), 8 s (dashed), and 14 s (dotted)
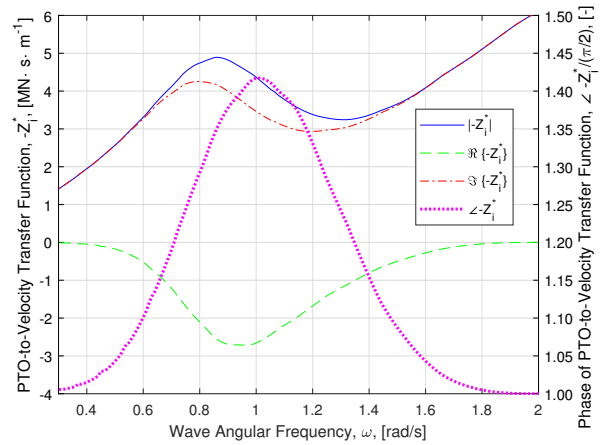

Fig. 5. Plot of the magnitude, real, imaginary component, and phase for PTO-to-Velocity transfer function

component of $-Z_3^*$ increases, as shown in Figure 6.

If the PTO and controller can maintain the optimal oscillation amplitude and phasing between the WEC velocity and the wave-excitation force, then the mechanical power input to the PTO will be maximised (Falnes (2002)). However, unless the mechanical-to-electrical efficiency is equal to unity, there will be losses when the PTO must achieve the commanded force at a given oscillation velocity (Falcao and Henriques (2015)). If the PTO mechanical-to-electrical efficiency is assumed to be time-invariant and independent of the PTO force magnitude, then the time-averaged power output can be calculated from the following set of equations:
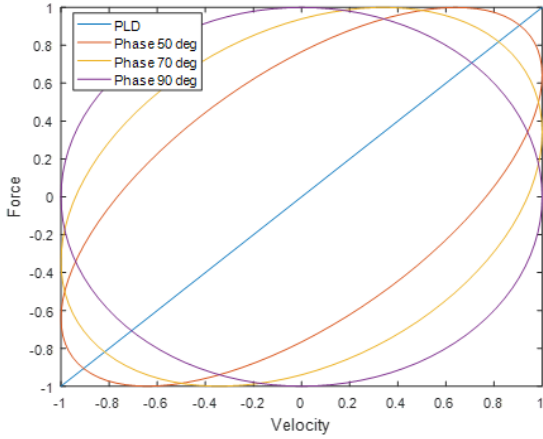
Fig. 6. Sketch of the changing relationship between velocity and force with changing phase angle
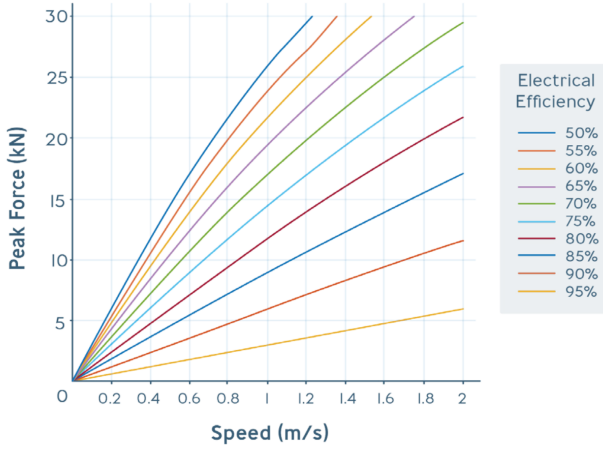

Fig. 7. PTO efficiency map between PTO force and speed for Trident Power-pod PTO

$$G = \left| \frac{\Im\{-Z_3^*(\omega)\}}{\omega\Re\{-Z_3^*(\omega)\}} \right| \ , \ G^* = \arctan G$$

$$P_O = \eta_e \frac{\Re\{-Z_3^*(\omega)\}\left|\dot{\zeta}_3(\omega)\right|^2}{2}\left[1 + e^*g^*\right] \qquad (19)$$

$$e^* = \frac{1 - \eta_e^2}{\eta_e} \qquad (20)$$

$$g^* = \frac{2G^* - \sin 2G^* - 2G\left(1 - \cos^2 G^*\right)}{2\pi} \qquad (21)$$

where η_e is the time and force invariant PTO mechanical-to-electrical efficiency. However, often the PTO efficiency varies depending on the operating condition of the WEC. A sample efficiency map of the Trident Power-pod PTO, designed for use with PLD, is plotted in Fig. 7.

If the efficiency of the PTO is not accounted for in the control strategy, then the energy capture of OVT methodologies can be severely degraded, with negative energy capture a real possibility (Genest et al. (2014)), as observed in Fig. 4. To highlight this issue, the power output after applying the efficiency map, shown in Fig. 7, was calculated from applying optimum OVT ($F_V = -Z_3^*$) and PLD ($F_V = -|Z_3|$) control strategies and over a range of values for the real and imaginary components of F_V in
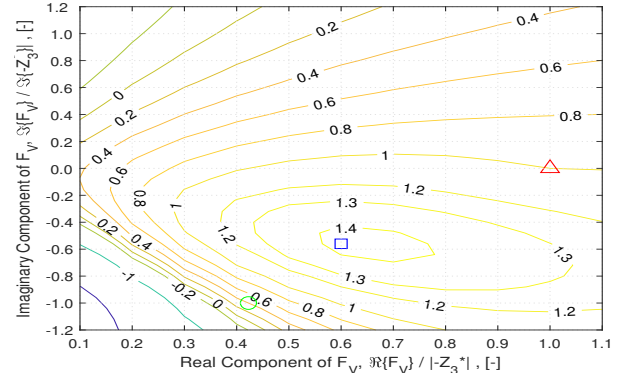

Fig. 8. Output power, relative to PLD, after accounting for the nonlinear PTO force and speed efficiency map for a wave period and height of 5 s and 1.0 m
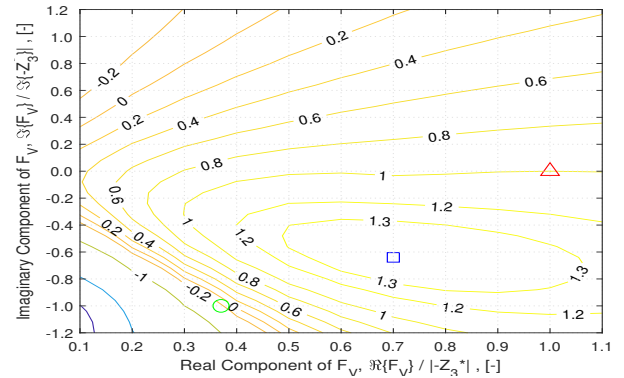

Fig. 9. Output power, relative to PLD, after accounting for the nonlinear PTO force and speed efficiency map for a wave period and height of 8.4 s and 1.0 m

regular waves, as shown in Fig. 8, Fig. 9, and Fig. 10. In each figure, there are three markers of interest: 1) the green circle represents the application of OVT without considering the PTO efficiency map, 2) the blue square represents application of an OVT methodology to maximise power capture when considering the PTO efficiency map, and 3) the red triangle represents the application of PLD. As observed from these figures, the blind application of OVT leads to reduced or even negative power capture. After considering the PTO efficiency, the power capture is increased by 30-60%; however, the more interesting result is that although the blind OVT moves left on the 2D map, when moving from a 5-s to 10-s wave period, the efficiency adapted OVT stays in approximately the same range of $0.6 < \Re\{F_V\}/|-Z_3^*| < 0.7$ and $\Im\{F_V\}/\Im\{-Z_3^*\} \approx 0.6$. In addition, the surface gradient about the optimum point is fairly flat, which means power capture gains will not drop dramatically if the real and imaginary components of $F_V(\omega)$ are not at the exact optimum point. The results from Fig. 8-10 allow for the calculation of a phase lag and amplitude modulation relative to the OVT motion trajectory to reach the optimum solution when including PTO efficiency. The phase lag and amplitude modulation can be included in a loop-up table to modify the reference trajectory, hence allowing OVT to adapt to PTO efficiency. A phase lag, ϕ, is introduced without changing the reference velocity magnitude (see Fig. 11). A 10-deg phase lag improves power capture but when moving to a 20-deg phase lag, as calculated from Fig. 10, the power capture is
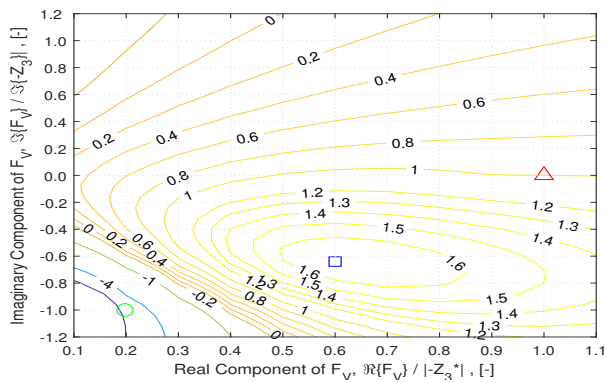
Fig. 10. Output power, relative to PLD, after accounting for the nonlinear PTO force and speed efficiency map for a wave period and height of 10 s and 1.0 m
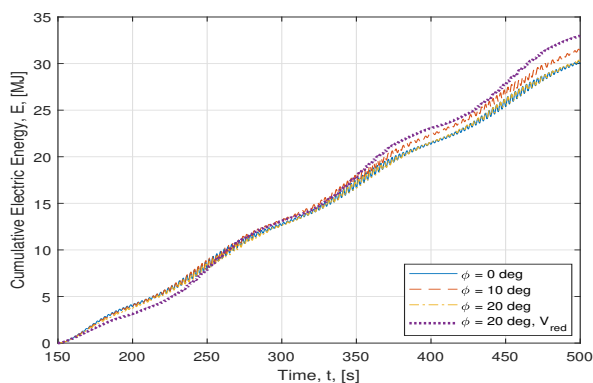

Fig. 11. Time series of electrical output energy after modifying the reference velocity trajectory for a wave period and height of 10 s and 1.0 m

reduced; however, once the amplitude modulation, A_{mod}, is included, a greater increase in power capture is observed. Therefore, the OVT methodology can potentially be adopted for PTO efficiency by implementing a phase lag and amplitude modulation that is calculated for a given efficiency map between the PTO force and speed. However, for this paper a specific regular wave scenario has been presented and full verification will require the generation of an amplitude and phase lag look up table that is tested in an irregular wave sea state.

5. CONCLUSION

In the work presented, improvements to aid implementation of OVT controllers are added. Limitations on acceleration are added, a new integral action is added to prevent positional drift when velocity and/or acceleration are limited, and an anti-wind up look to prevent controller saturation is added. The work presented highlights the issues in implementing impedance matching control methodologies to point absorber WECs. Specifically:

- Whilst the movement and force can be constrained to set limits, the latter has a detrimental effect upon the former as large forces are sometimes be required to limit the movement of the WEC.
- Force limitations and PTO efficiency can have a highly detrimental effect on energy capture using

impedance matching; in some cases causing, the WEC to consume energy.

The second point listed was demonstrated for regular waves with a maximum peak improvement for OVT considering efficiencies identified. Interestingly, the optimal operational point does not vary greatly with the wave period and the surface gradient is fairly flat. This result shows that a controller that provides reactive as well as active power could still outperform a linear damping approach, development of which would be an interesting area for further work. The work presented also makes a clear case for co-design of control and the WEC/PTO system. Whilst the PTO used is well designed for linear damping control, it is often forced to operate away from its most efficient force-speed curve. The total force for impedance matching is also much higher than the maximum force for large waves. Co-design is clearly essential for well-designed WEC and PTO combinations using impedance matching methodologies and attempting to apply impedance matching control to WEC and PTO combinations designed for linear damping may be fraught with difficulty.

REFERENCES

Coe, R., Bacelli, G., Wilson, D., Abdelhkalik, O., Korde, U., and Robinett III, R. (2017). A comparison of WEC control strategies. *International Journal of Marine Energy*, 20, 45–63. doi:10.1016/j.ijome.2017.11.001.

Evans, D. (1976). A theory for wave-power absorption by oscillating bodies. *Journal of Fluid Mechanics*, 7(1), 1–25. doi:10.1017/S0022112076001109.

Evans, D. (1981). Maximum wave-power absorption under motion constraints. *Applied Ocean Research*, 3(4), 200–203. doi:10.1016/0141-1187(81)90063-8.

Falcao, A. and Henriques, J. (2015). A simple and effective real-time controller for wave energy converters. *Journal of Ocean Engineering and Marine Energy*, 1(1), 1–14. doi:10.1007/s40722-015-0023-5.

Falnes, J. (2002). *Ocean waves and oscillating systems: linear interactions including wave-energy extraction*. Cambridge University Press.

Fusco, F. and Ringwood, J.V. (2013). A simple and effective real-time controller for wave energy converters. *IEEE Transactions on Sustainable Energy*, 4(1), 21–30. doi:10.1109/TSTE.2012.2196717.

Genest, R.and Felician, B., Clement, A., and Babarit, A. (2014). Effect of non-ideal power take-off on the energy absorption of a reactively controlled one degree of freedom wave energy converter. *Applied Ocean Research*, 48, 236–243. doi:10.1016/0141-1187(81)90063-8.

Hals, J., Falnes, J., and Moan, T. (2011). A Comparison of Selected Strategies for Adaptive Control of Wave Energy Converters. *Journal of Offshore Mechanics and Arctic Engineering*, 133(3), 031101. doi:10.1115/1.4002735.

Ringwoord, J., Bacelli, G., and Fusco, F. (2014). Energy-maximizing control of wave-energy converters: The development of control system technology to optimize their operation. *IEEE Control Systems Magazine*, 34(5), 30–55. doi:10.1109/MCS.2014.2333253.

Stock, A., Gonzalez, C., and Robb, D. (2018). Final Stage 2 Project Report - IMPACT. Technical report, SgurrControl (part of Wood), Glasgow.

Trident Energy (2014). PowerPod Technical Datasheet. Technical report, Trident Energy.